JOURNAL OF AGRICULTURAL AND FOOD CHEMISTRY

J. Agric. Food Chem. **2007,** *55,* 7905–7915 **7905**

Characterization of Protein Changes Associated with Sugar Beet (*Beta vulgaris*) Resistance and Susceptibility to *Fusarium oxysporum*

REBECCA L. LARSON,*,† AMY L. HILL,† AND ALBERTO NUÑEZ‡

Sugarbeet Research Unit, Agricultural Research Service, U.S. Department of Agriculture, 1701 Centre Avenue, Fort Collins, Colorado 80526, and ERRC, Agricultural Research Service, U.S. Department of Agriculture, 600 East Mermaid Lane, Wyndmoor, Pennsylvania 19038

Fusarium oxysporum (F-19) is a serious threat to sugar beet. Resistance exists, but the basis for resistance and disease is unknown. Protein extracts from sugar beet genotypes C1200.XH024 (resistant, R) and Fus7 (susceptible, S) were analyzed by multidimensional liquid chromatography at 2 and 5 days postinoculation (dpi) and compared to mock-inoculated controls. One hundred twenty-one (R) and 73 (S) protein peaks were induced/repressed by F-19, approximately 12 (R) and 8% (S) of the total proteome detected. Temporal protein regulation occurred within and between each genotype, indicating that the timing of expression may be important for resistance. Thirty-one (R) and 48 (S) of the differentially expressed peaks were identified using matrix-assisted laser desorption–ionization with tandem time-of-flight mass spectrometry; others were below detection level. Comparison between the two genotypes uncovered R- and S-specific proteins with potential roles in resistance and disease development, respectively. Use of these proteins to select for new sources of resistance and to develop novel disease control strategies is discussed.

KEYWORDS: Sugar beet; plant defense; *Fusarium oxysporum*; subtractive proteomics; multidimensional liquid chromatography; *Beta vulgaris*

INTRODUCTION

Plants have a variety of mechanisms for defending themselves against pathogens. Induced defense responses are correlated with coordinated expression of several classes of proteins including proteins with antimicrobial and antioxidant properties and cell-signaling functions (*1*, *2*). The most common and best-characterized group of induced proteins includes the 17 families of pathogenesis-related (PR) proteins (*3*). In addition to novel protein expression, induction of resistance is often correlated with a change in metabolism, including respiration (*4*).

Genomics is currently the most prevalent approach for studying host resistance (*5*, *6*). Although quite informative, correlation between transcript and protein does not always exist (*7*). The difference is based on protein regulation through compartmentalization (*8*), modification (*9*), and interaction with other cellular constituents (*10*) following transcript expression. These phenomena can only be fully examined using proteomics.

Two-dimensional electrophoresis (2DE) is the backbone of traditional proteomics. However, many proteins have historically been underrepresented using this fractionation technology (*11*). In comparison to traditional isoelectric focusing, ion exchange chromatography (IEX) allows for greater protein identification with higher confidence (*12*). Combining IEX with reversed phase high-performance liquid chromatography (RP-HPLC) is termed multidimensional liquid chromatography (MDLC). Chromatographic approaches provide higher resolution and reproducibility as well as unparalleled levels of sensitivity when compared to 2DE (*13*, *14*) and are reliably quantitative (*15*). Subtractive comparison of proteomic data generated by MDLC is a quick and reproducible method for identifying proteins unique to a particular physiological condition.

Fusarium oxysporum, the causal agent of Fusarium Yellows of sugar beet, is a serious threat to sugar beet production worldwide. Although several lines of sugar beet appear to have resistance to the fungus, the basis for resistance is not well-understood. The variability in the pathogen population is large (*16*), and the response of sugar beet to *Fusarium* is isolate-specific; furthermore, the efficacy of the resistant genotypes varies by geographical location (S. Godby, personal communication). This is complicated by the fact that identification of new sources of resistance can be a laborious task, since identification is largely empirical. In the current investigation, we examine protein changes in resistant and susceptible sugar beet germplasm following inoculation with *F. oxysporum*. Gaining a better understanding of host changes associated with resistance and susceptibility will provide a framework for

* To whom correspondence should be addressed. Tel: 970-492-7141 . Fax: 970-492-7160. E-mail: Rebecca.larson@ars.usda.gov.
† Sugarbeet Research Unit.
‡ ERRC.

10.1021/jf070876q
Published on Web 08/23/2007

identifying markers for resistance selection and the development of more advanced disease control strategies.

MATERIALS AND METHODS

Plant Culture. Sugar beet (*Beta vulgaris* line C1200.XH024, resistant to *F. oxysporum* isolate F-19, provided by American Crystal Sugar Co., Moorhead, MN; *B. vulgaris* line Fus7, susceptible for *F. oxysporum* isolate F-19, provided by KWS Saat Ag, Einbeck, Germany) was seeded into 20 cm diameter pots containing pasteurized (3 h at 72 °C and 0.4 Bar) Metro-Mix 200 (The Scotts Co., Marysville, OH). At 2 weeks postemergence, seedlings were transplanted (three per pot) into 20 cm pots. Plants were maintained in a glasshouse at 22 ± 5 °C, watered daily, and kept under 16 h of daylight to maintain vigorous growth.

Fungal Culture. A stock culture of *F. oxysporum* isolate F-19, a highly virulent *Fusarium* isolate (*17*), was maintained on potato dextrose agar (PDA, Becton, Dickinson and Co., Sparks, MD) at 25 ± 2 °C with 8 h of supplemental light per day. *Fusarium* inoculum was prepared by transferring a 4 mm plug of fungal hyphae from the actively growing edge of a fungal colony on PDA to half strength V8 agar. Plates were incubated under 8 h light/16 h dark at 22–25 °C for 2 weeks. Hyphal material and spores were harvested from 24 plates into sterile distilled water (7.5 mL per plate) by scraping with a sterile cell spreader and then strained through sterile cheesecloth. The spore concentration was determined with a hemacytometer and adjusted to approximately 1×10^5 conidia mL^{-1}.

Plant Inoculation. Six week old plants (10 plants per treatment per sampling time) were removed from soil and rinsed under running tap water. Roots were soaked in the F-19 spore suspension or sterile water (mock inoculation) for 8 min with intermittent agitation and then replanted into a 20 cm pot, arranged in a completely randomized design, watered daily, and maintained at 26–28 °C. At 2 and 5 days postinoculation (dpi), 10 sugar beets per treatment were gently removed from the soil, rinsed under running tap water, and then blotted dry. Two and five days corresponded with initial fungal penetration and vascular tissue penetration, respectively (Linda Hanson, personal communication). Plants were separated into root and leaf fractions, ground in liquid nitrogen, lyophilized (−80 °C for 48 h), and stored at −80 °C until extraction. The experiments were repeated on two independent occasions.

Protein Extraction. For protein extraction, approximately 2.5 g each of leaf and root material was extracted separately using the plant fractionated protein extraction kit (Sigma, St. Louis, MO) according to the manufacturer's recommendations. The protein concentration was determined by Bradford assay (Bio-Rad, Hercules, CA) using bovine serum albumin standards (0–20 μM). Leaf and root proteins were pooled (3:1, 2.0 mg of leaf protein to 0.7 mg of root protein). In preparation for fractionation by MDLC, protein was exchanged into start buffer (Beckman Coulter, Fullerton, CA) using a PD-10 desalting column (GE Healthcare, Piscataway, NJ) according to the manufacturer's recommendations. Following the buffer exchange, the final protein concentration was determined with a BCA Protein Assay kit (Pierce Biotechnology, Rockford, IL). Equal amounts of protein were injected into the MDLC each run to facilitate comparisons between the relative abundance of each protein peak in downstream analyses.

Proteome Analysis by MDLC. Proteins were separated using ProteomeLab PF2D, two-dimensional protein fractionation system (Beckman Coulter) according to the manufacturer's recommendations. Briefly, first-dimension separation (IEX) was carried out with a PF2D HPCF column (250 mm × 2.1 mm) (Beckman Coulter) over 220 min at room temperature (flow rate of 0.2 mL min^{-1}) over a pH gradient of 4.0–8.5. The protein presence was monitored real time by measuring the absorbance at 280 nm. Fractions from the first dimension separation were collected in 0.3 pH unit intervals using an FC/I module (Beckman Coulter). Fractions outside the gradient were collected by time (5 min per fraction). Fractions collected during the first-dimension separation were further separated by RP-HPLC (500 μL injection volume for each fraction) on a nonporous C18 PF2D HPRP (46 mm × 3.3 mm) (Beckman Coulter) column maintained at 50 °C with a flow rate of 0.75 mL min^{-1}. The column gradient began with 0.1% trifluoroacetic acid (TFA) in nanopure water and progressed towards 0.08% TFA in acetonitrile over 35 min. At the conclusion of the gradient, the column was washed for 4 min with 0.08% TFA in acetonitrile before re-equilibrating with 0.1% TFA in nanopure water for 8 min. Protein fractions from each second-dimension separation were collected in a series of eight 96-well plates (0.5 mL per well). Protein peaks were detected by absorbance at 214 nm. Protein plates were sealed and stored at −80 °C until the time of analysis.

Subtractive Proteomics. Proteins induced or repressed by F-19 in the susceptible and resistance genotype were identified using subtractive proteomics. The chromatographs obtained during the second-dimension fraction for each treatment (mock- and F-19-inoculated), genotype source (line C1200.XH024 or Fus7), time point (2 and 5 dpi), and biological replicate were aligned using the 32 Karat software (Beckman Coulter). Differentially expressed proteins (qualitative and quantitative; induced or repressed in relation to the mock-treated control) were assigned a peak number for identification. The protein peak had to be reproducibly detected in both independent experimental replicates (for either, stage-specific, or both, pathogen-specific, time points) to be considered nonartifacts. The relative abundance of the identified peaks was determined by averaging the integration value (area under the peak) of the selected protein peaks for each biological replicate, sampling time, and treatment. The fractions containing peaks of interest were transferred to a sterile 2 mL tube prerinsed with acetonitrile. Protein fractions were frozen, dried using a CentriVap concentrator (Labconco, Kansas City, MO), and then resuspended in 50 μL of 50 mM ammonium bicarbonate, pH 8.0, and digested with trypsin (Promega, Madison, WI) overnight at 37 °C. Following trypsin digestion, trifluoroacetic acid was added to each sample at a final concentration of 0.2% (v/v) to terminate the digestion and acidify the sample. The resultant peptides were purified and concentrated on C18 ZipTip pipette tips (Millipore, Brillerica, MA) according to the manufacturer's recommendations. Eluted peptides were diluted 1:1 in matrix (α-cyano-4-hydroxy-cinnamic acid, 5 mg mL^{-1}, Bruker Daltonics, Billerica, MA) and spotted in duplicate onto stainless steel matrix-assisted laser desorption–ionization (MALDI) plates (Applied Biosystems, Foster City, CA).

Protein Identification. MALDI mass spectrometry with automated tandem time of flight fragmentation of selected ions (MALDI-TOF/TOF) of trypsin-digested proteins was acquired with a 4700 Proteomics Analyzer mass spectrometer (Applied Biosystems, Framingham, MA) in the positive reflectron mode with a 200 Hz Nd-YAG 355 nm laser. Spectra were obtained by averaging 1000 and 2500 acquired spectra in the MS and MS/MS mode, respectively. Collision-induced dissociation (CID) with air at an approximately 1×10^{-6} Torr and a 1 keV acceleration voltage was used for obtaining the MS/MS spectra for selected peptides. Conversion of TOF to mass (Da) for the monoisotopic ions, $[M + H]^+$, was based on calibration of the instrument with a peptide standard calibration kit (Applied Biosystems) that contained the following peptides: des-Arg^1-bradykinin (*m/z* 904.4681), angiotensin I (*m/z* 1296.6853), Glu^1-fibrinopetide B (*m/z* 1570.6774), ACTH (clip 1–17) (*m/z* 2903.0867), ACTH (clip 18–39) (*m/z* 2.465.1989), and ACTH (clip 7–38) (*m/z* 3657.9294). Calibration of TOF for MS/MS mode was obtained from the CID-produced fragments of Glu^1-fibrinopetide B. Peptide mass fingerprints and MS/MS spectra for each sample were combined and queried against the primary sequence database using the Mascot (Matrix Science, Inc. Boston, MA) search engine through GPS Explorer Software (Applied Biosystems) with a 50 ppm and 0.1 Da error tolerance for MS and MS/MS spectra, respectively, one missed trypsin cleavage allowance, and oxidation of methionine as a variable modification. The signal to noise ratio for peak filtering was set to 10 for MS and 20 for MS/MS. Additional database searches were conducted with lone MS/MS spectra of the selected peptides. Reported proteins from database searches (MS + MS/MS and MS/MS) from putative peptide sequences were within a ≥95% confidence interval ($P > 0.05$). De novo sequencing of unidentified peptides was accomplished by MS/MS spectrum interpretation using PEAKS (Bioinformatics Solutions Inc., Waterloo, Ontario, Canada) automatic de novo algorithm software (*18*), with the following parameters: precursor ion mass tolerance, 0.05 Da; fragmented ions mass tolerance, 0.1 Da; and trypsin as the digestion enzyme. Oxidized

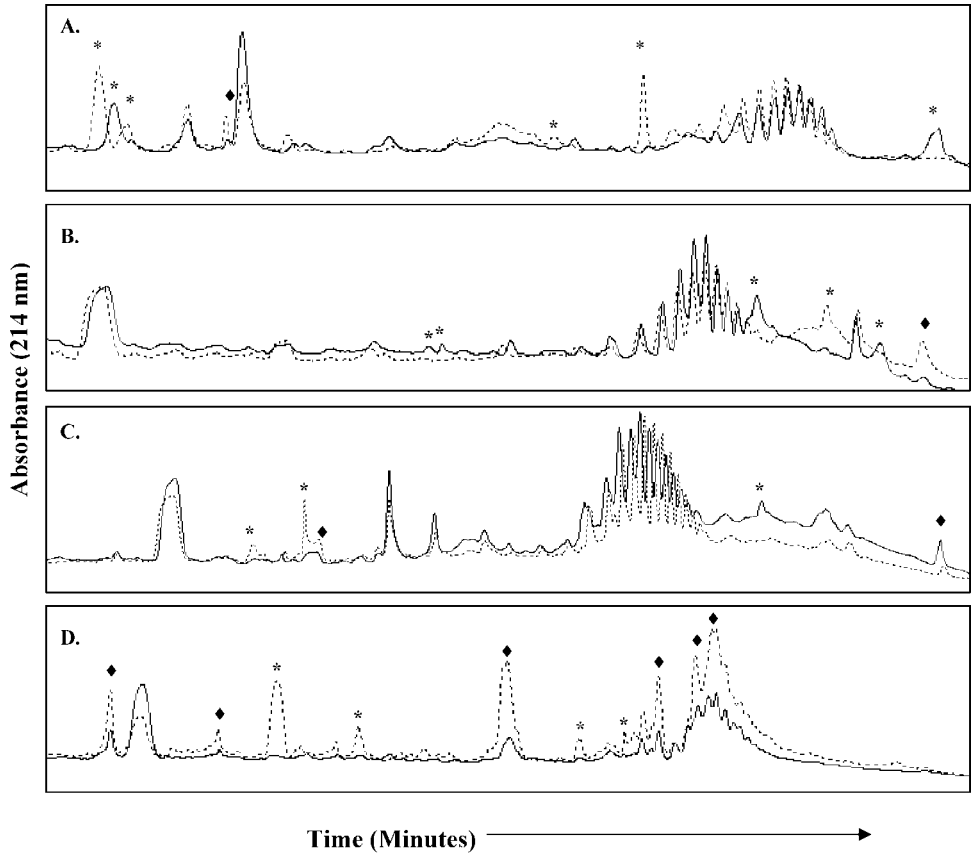

Figure 1. Representative protein chromatograms from fungal- (dashed line) and mock (solid line)-inoculated tissue as detected in the second dimension (RP-HPLC) separation of MDLC are provided to show accuracy of alignment for detection of significant quantitative (diamond) and qualitative (asterisk) differences between treatments. Peak alignments are from the resistant genotype (C1200.XH024) at 2 (**A**; fraction 32, 12.5–20.0 min) and 5 (**B**; fraction 20, 12.5–20.5 min) dpi, and the susceptible genotype (Fus7) at 2 (**C**; fraction 32, 12.0–21.5 min) and 5 (**D**; fraction 9, 12.5–20.5 min) dpi. On average, 87% of the differentially expressed peaks were detected between experimental replicates, which indicates low biological variability and a high degree of technical reproducibility.

methionine was selected as a variable modification, and de novo sequences carrying methionine were verified by detection of the oxidized/nonoxidized ion in the MS spectrum, which provided additional confirmation. Homology-based searches using NCBI's basic local alignment search tool were limited to Viridiplantae (all green plants) using the nonredundant database option and PAM30 score matrix. The peptide sequence used for each search was limited to amino acids deduced with greater than 90% confidence and stretches consisting of greater than five amino acids. The error for isobaric amino acids was taken into consideration. All protein assignments, regardless of identification method (MS + MS/MS, MS/MS alone, or PEAKS), were further validated by examining the degree of homology of the peptide sequence across five species.

Protein Characterization and Classification. All proteins identified in this study were classified according to biological role under the following categories: oxidative response (Ox), photosynthesis (PS), defense-related (Def), stress response (SR), gene/protein expression (Exp), primary or secondary metabolism (Met), cell development (CD), signal transduction (ST), or not determined (ND) based on experimental evidence from the literature, information in the gene bank submissions, and using the gene ontology program AmiGO (http://www.godatabase.org). The subcellular location was predicted for all proteins identified in this study using TargetP v. 1.1 (http://www.cbs.dtu.dk/services/TargetP), according to Zhou et al. (*19*). For those proteins predicted to be located in organelles or secreted, transit and secretion signal peptide locations were predicted using ChloroP v. 1.1 (http://www.cbs.dtu.dk/services/ChloroP), MITOPROT (http://ihg.gsf.de/ihg/mitoprot.html), or SignalP v. 3.0 (http://www.cbs.dtu.dk/services/SignalP) for chloroplastic, mitochondrial, and secreted proteins, respectively. Following this prediction, the signaling and transit peptide sequences were removed, and the resultant isoelectric point was calculated using ExPASy's compute pI/Mw tool (http://www.expasy.org/tools/pi_tool.html).

RESULTS

Protein Expression Is Temporally Regulated. Protein analysis using MDLC was highly reproducible, 85–91% between biological replicates (**Figure 1**); therefore, there was low variability amounting to 9–15%. Analysis of protein expression in sugar beet at 2 dpi (initial fungal penetration) and 5 dpi (vascular tissue penetration) showed that proteins are temporally regulated during resistance and disease. In the resistant and susceptible genotypes, a total of more than 950 unique peaks were reproducibly detected in the protein extracts from each treatment. Some stage-specific protein changes were observed in both genotypes. In the resistant line, 14 protein peaks were affected by F-19 at 2 dpi but not 5 dpi. Likewise, 43 protein peaks were affected by F-19 at 5 dpi but not 2 dpi. In the susceptible line, 14 protein peaks were affected by F-19 at 2 dpi and not 5 dpi, while 22 protein peaks were affected by F-19 at 5 dpi and not 2 dpi. Some proteins were affected by the fungus at both time points, including 49 induced and 15 repressed in the resistant line at both 2 and 5 dpi and 14 induced and 23 repressed in the susceptible line at both time points. Thirty-three peaks had similar expression patterns in both genotypes, suggesting that they were unrelated to the resistance or disease phenotype, leaving 40 susceptibility-specific and 88 resistant-specific peaks. The change in protein expression following F-19

Table 1. Proteins in Sugar Beet Affected by Challenge with *F. oxysporum* Isolate F-19 as Identified Using Combined MS + MS/MS Data

peak no.	protein name	pI (obs/exp)[a]	no. of peptide matches	% sequence coverage[b]	peptide(s) matches[c]	accession no.	cellular location[d]	role[e]	R2[f]	R5[f]	S2[f]	S5[f]
					resistant germplasm							
1	OEC 16 kDa subunit	>8.5/9.66(9.32)	2	6	FYIQPLSPTEAAQR	O22591	CP (73/74)	Ox	ND	+	ND	ND
5	water-oxidizing complex 33 kDa polypeptide	4.78–4.96/5.89(5.28)	6	33	RLTFDEIQSK DGIDYAAVTVQLPGGER QLVASGKPESFSGEFLVPSYR	505482	CP (930/31)	Ox	+	+	ND	ND
6	chitinase	>8.5/8.82(8.81)	4	86	FGYCGVGR SGECNMYGR	E1265996	S (28/29)	Def	+	+	+	+
11	OEC 16 kDa subunit	>8.5/9.66(9.48)	3	15	FYIQPLSPTEAAQR	58700507	CP (47/48)	Ox	+	+	ND	ND
12	ubiquitin	>8.50/6.56	3	46	ESTLHLVLRL IQDKEGIPPDQQR	P42739	O	Exp	+	ND	ND	ND
14	glutathione-S-transferase	>8.5/6.09	6	23	VLDVYEAR	Q96266	O	Ox	+	+	ND	ND
18	hypothetical protein	>8.5/8.66	5	64	GGECYDPVMPLTSR	50725661	O	ND	+	+	–	–
19	allergen	<4.0/5.52(5.46)	10	23	FNLAGNHEQEFLR	Q6T2T4	S (20/21)	Def	+	+	ND	ND
21	superoxide dismutase (SOD)	5.87–6.14/5.46	2	14	AVVVHADPDDLGR	P93258	O	Ox	+	+	ND	ND
22	PR1a precursor	5.56–5.87/5.78(5.28)	3	24	SVRLGCAR	Q08697	S (21/22)	Def	+	+	ND	ND
24	50S ribosomal protein L12	4.48–4.78/5.50(4.62)	2	16	TEFDVSIDEVPSNAR IEQLGTQLSGLTLEEAR	P02398	CP (56/57)	Exp	+	+	ND	ND
25	TSI-1	4.18–4.48/5.61	6	48	IHVIDDK	2887310	O	Def	ND	+	ND	ND
26	polyphenol oxidase (PPO)	3.88–4.18/5.90	2	6	TQTEYAGSFVNVPHR	Q40775	O	Ox	ND	+	ND	ND
90	rubisco LSU	<4.0/6.78	3	7	TPEYETLDTDILAAFR	Q9MTG1	O	PS	+	ND	–	–
187	thioredoxin H-type 1	5.26–5.56/5.23	2	16	FIAPILADLAK	P29449	O	Ox	+	+	+	ND
191	50S ribosomal protein L12	4.96–5.26/5.50(4.62)	4	36	TEFDVSIDEVPSNAR IEQLGTQLSGLTLEEAR	TC1038	CP (56/57)	Exp	+	+	–	–
206	rubisco LSU	5.56–5.87/6.13	6	23	DITLGFVDLLR TFQGPPHGIQVER	AAQ75613	O	PS	+	+	–	ND
210	50S ribosomal protein L12	4.18–4.48/5.50(4.62)	3	32	IEQLGTQLSGLTLEEAR	TC1038	CP (56/57)	Exp	+	+	ND	ND
					susceptible germplasm							
37	cyclophilin A, B and H-like	4.93–5.23/8.32(5.69)	1	6	VFFDVDIGGEPVGR	AAG40378	CP (77/78)	Exp	ND	ND	+	+
38	rubisco activase	4.93–5.23/8.61(5.81)	8	14	IVDSFPGQSIDFFGALR	AAC15236	CP (58/59)	PS	ND	ND	–	–
39	peroxidase 43 precursor	4.91–5.21/5.68(5.36)	3	11	NAFGHEGVR	Q9SZH2	S (24/25)	Def	+	ND	+	+
100	actin binding protein	>8.5/5.35	24	15	EHEAKLDEAGDLQR GELEVLLFTLQSAMRANNQRPFVPR EWATQLENEMTREDQPADLTTVNVAMQK	CBG19038	O	CD	ND	ND	ND	+
102	H+-transporting two-sector ATPase	>8.5/4.44	4	43	SEDADAALSGLVEFLEEK	T06998	O	Met	+	+	–	–
107	tonoplast aquaporin TIP5.1	>8.5/7.04	3	33	AYFAEFFSTFLFVFIAVGSTISAR	Q7XU31	O	SR	ND	ND	+	+
109	rubisco LSU	8.19–8.35/6.29	2	7	DITLGFVDLLR	Q8SMA9	O	PS	ND	ND	+	+
114	receptor-like kinase	6.40–6.70/6.25	4	10	LVMQYLCGDVLLPAMPESYR	Q7F165	O	ST	–	–	–	–
116	peroxisome assembly protein	6.09–6.40/7.99	2	15	QHPTETPCGHVFCWSCIMEWCNEK	T00968	O	Ox	ND	ND	–	–
119	rubisco LSU	5.23–5.53/6.73	10	19	DITLGFVDLLR TFQGPPHGIQVER	Q33420	O	PS	ND	ND	–	–
122	BZIP TF ATB2	5.07–5.37/6.13(5.16)	2	35	none	Q8L5W2	CP (25/26)	Exp	ND	ND	–	–
126	OEC protein 1 precursor	5.07–5.37/6.26(5.30)	3	11	VPFLFVK QLVASGKPESFSGEFLVPSYR	T06368	CP (27/28)	Ox	ND	ND	+	+
128	rubisco LSU	4.76–5.07/6.78	3	9	TPEYETLDTDILAAFR	Q9MTG1	O	PS	ND	ND	+	+
129	OEC 33 kDa subunit	4.76–5.07/5.63(5.16)	2	7	QLVASGKPESFSGEFLVPSYR VPFLFVK	S11852	CP (29/30)	Ox	ND	ND	+	ND
129	ATP synthase D chain	4.76–5.07/5.19	12	67	FSQEPEPIDWEYYR	AAM16192	O	Met	ND	ND	+	ND

Table 1. Continued

peak no.	protein name	pI (obs/exp)[a]	no. of peptide matches	% sequence coverage[b]	peptide(s) matches[c]	accession no.	cellular location[d]	role[e]	R2[f]	R5[f]	S2[f]	S5[f]
642	rubisco	4.03–4.14/6.13	9	32	DITLGFVDLLR TFQGPPHGIQVER GGLDFTKDDENVNSQPF LTYYTPEYETLDTDILAAF	AAQ75613	O	PS	+	+	ND	+

[a] The observed isoelectric point (pI) was derived from the first dimension report obtained during MDLC fractionation. The expected pI was determined using ExPASy's Compute pI/MW tool. The pI was not able to be determined for expressed sequence tag (EST) match (ND), and the pI was recalculated following removal of chloroplast transit peptide and secretion signal sequence when appropriate; the processed protein pI is shown in parentheses. [b] Sequence converage was determined by matching theoretical data corresponding to the identified proteins with the experimental data from the corresponding spots. [c] Peptide sequence matches are only listed for parent ions that had significant (>95% C.I.) MS/MS scores. In cases where matches were significant for PMF data alone, "none" is listed. [d] The cellular location of the identified protein was determined using TargetP v. 1.1. Location designations: CP, chloroplast; O, other; S, secreted; and ND (EST), not determined for EST. Numbers in parentheses represent cleavage sites for chloroplast transit peptides or secretion signals as determined with ChloroP v. 1.1 and SignalP v. 3.0, respectively. [e] Biological role of the identified protein: Ox, oxidative; PS, photosynthesis; Def, defense; SR, stress response; ST, signal transduction; Exp, gene/protein expression; Met, primary/secondary metabolism; CD, cell development; and ND, not determined. [f] Relative expression in comparison to mock-inoculated control for resistant line at 2 (R2) and 5 dpi (R5) and susceptible line at 2 (S2) and 5 dpi (S5). Increased expression (induction), +; decreased expression (repression), –; and no difference in expression level, ND.

inoculation represents approximately 12 and 8% of the total proteins detected with MDLC for the resistant and susceptible genotype, respectively.

Protein Characterization. Of the 121 total protein fractions containing differentially expressed peaks from the resistant genotype, 51 peaks eluted at concentration levels that make identification with MALDI-TOF/TOF mass spectrometry difficult; therefore, only 70 were subjected to further analysis. Similarly, only 48 of the 73 differentially expressed peaks in the susceptible genotype were at levels conducive to analysis by MALDI-TOF/TOF. Sugar beet is not well-represented in public databases; therefore, several approaches were necessary for protein identification. For all proteins, first attempts at protein assignment were completed using Mascot analysis software searching with combined peptide mass fingerprint and MS/MS spectra (**Table 1**). Additional identification with Mascot was achieved by running MS/MS spectra individually against the nonredundant database (**Table 2**). Lastly, identification of the remaining proteins was attempted through homology-based searching with the de novo peptide sequence derived from the MS/MS spectra using PEAKS (**Table 3**). Using all three approaches, 31 (resistant genotype) and 48 (susceptible genotype) proteins were identified with greater than 90% confidence. All protein identifications were furthered validated by comparing the degree of homology of the peptide sequence across five diverse plant species (data not shown). Furthermore, proteins identified with single peptide matches were only accepted if the matched sequence was located within a highly conserved functional domain as determined using NCBI's conserved domain database (data not shown). The accession number for the protein that was the best fit match is provided for each peak. Sequence coverage was determined by dividing the number of amino acids spanned by the assigned peptides by the total sequence length of the best fit match. The total number of peptide matches was computed by tallying the total number of primary peptide sequences assigned to the protein. Peptides with the same sequence that represent different charge or modification states were only counted once. The isoelectric point for the best fit match was determined in silico from the amino acid sequence.

Oxidative Proteins. Several proteins affected in beet by F-19 are associated with generation and detoxification of reactive oxygen species and the oxidative reactions in photosynthesis. Mascot searches of MS + MS/MS spectra identified the following: oxygen-evolving complex (OEC; #1, #11, #126, #129), water-oxidizing complex (#5), glutathione-S-transferase (#14), SOD (#21), PPO (#26), thioredoxin (#187), and a peroxisome assembly protein (#116, **Table 1**). Searches of MS/MS spectra alone identified two more OECs (#7, #128) and a quinone oxidoreductase (#10, **Table 2**). Lastly, homology-based searches using PEAKS-derived amino acid sequences identified catalase (#115, **Table 3**). The relative abundance of resistance- (**Figure 2**) and susceptibility- (**Figure 3**) associated oxidative proteins was determined.

Photosynthesis Proteins. The proteins related to photosynthesis were identified as follows: rubisco large subunit (#90, #109, #119, #128, #206, #642), a common artifact in plant proteomics studies, and rubisco activase (#38, **Table 1**).

Defense Proteins. Proteins identified that have been correlated with resistance in other plant systems were categorized as defense proteins. Several proteins identified using MS + MS/MS can be categorized as PR proteins, including: chitinase (#6), PR1a (#22), TSI-1 (#25), and peroxidase (#39, **Table 1**). The allergen related to legumin, profiling and glycinin (#19, **Table**

Table 2. Proteins in Sugar Beet Affected by Challenge with *F. oxysporum* Isolate F-19 as Identified Using MS/MS Spectra Alone

peak no.	protein name	pI (obs/exp)[a]	peptide(s) matches[b]	accession no.	cellular location[c]	role[d]	R2[e]	R5[e]	S2[e]	S5[e]
			resistant germplasm							
4	PPR-repeat protein	>8.5/8.14 (8.69)	MVFETMIGR	Q6Z749	CP (48/49)	Exp	+	ND	ND	ND
7	OEC 16 kDa subunit	>8.5/9.66(9.32)	FYIQPLSPTEAAQR	AAB81994	CP (73/74)	Ox	+	+	ND	ND
10	quinone oxidoreductase	<4.0/4.84	NLDFIQAAALPLAIETAYEGLER	BAB50156	O	Ox	+	ND	ND	ND
15	receptor-like protein kinase	>8.5/5.75 (5.76)	VVSLSIPR	H84421	S (20/21)	ST	ND	+	ND	+
88	biotin carboxylase	6.74–7.04/7.22 (5.77)	LVSLLXLR	O23960	CP (76/77)	Met	+	ND	ND	ND
182	β-fructofuranosidase	4.18–4.48/4.98	LHGWGPMGFGGLLSGR	Q8VXS6	O	Met	+	+	ND	ND
192	TPR domain protein	4.96–5.26/5.02	LXLHLPR	Q602H7	O	Def	+	+	ND	ND
209	phosphoglycerate mutase	>8.5/8.81	ATISLLPR	P00950	O	Met	ND	+	ND	ND
			susceptible germplasm							
43	β-glucanase	<4.0/7.03 (7.18)	DHXISLLLR	Q9FHX5	S (26/27)	Def	+	+	ND	+
43	EST beet storage root	<4.0/ND	XHIFTLLAKVR	BQ589216	ND	ND	+	+	ND	+
101	99.7 kDa hypothetical protein F508.27	>8.5/9.44	SPPPPYVYSSPPPPPYYSPSPK	C86371	O	ND	ND	ND	+	ND
103	*B. vulgaris* root EST	>8.5/ND	SGELSXMVINGR	BI698288	ND	ND	ND	ND	–	–
105	hypothetical protein	>8.5/8.86	IVTVSCSR	Q8GYE5	O	ND	+	+	+	+
105	chitinase	>8.5/9.96(8.84)	YXASSLPR	Q9SC03	S (25/26)	Def	+	+	+	+
108	60S ribosomal protein L27	>8.5/9.06	LVSSLIXK	P41101	O	Exp	–	–	ND	+
124	elongation Factor 1a	5.07–5.37/9.19	IXLLVPPR	Q8GV27	O	Exp	–	–	–	–
128	OEC protein 1	4.62–4.93/5.89 (5.28)	QLVASGKPESFSGEFLVP	T02066	CP (30/31)	Ox	ND	ND	+	+
131	hypothetical protein	<4.0/5.81	NTGPISXR	Q7S784	O	ND	ND	ND	+	ND
639	*B. vulgaris* root EST	4.03–4.14/ND	ILAXEAPR	BQ589852	ND	ND	ND	ND	+	+
639	syringopeptin synthetase C	4.03–4.14/5.78 (5.61)	RLDALPR	Q3JM57	CP (49/50)	Def	ND	ND	+	+

[a] The observed isoelectric point (pI) was derived from the first dimension report obtained during MDLC fractionation. The expected pI was determined using ExPASy's Compute pI/MW tool. The pI was not able to be determined for EST match (ND), and the pI was recalculated following removal of mitochondrial transit peptide sequence when appropriate; the processed protein pI is shown in parentheses. [b] Denotes the peptide sequence with significant match (>95% C.I.) to MS/MS spectra. [c] The cellular location of the identified protein was determined using TargetP v. 1.1. Location designations: CP, chloroplast; O, other; S, secreted; and ND, not determined for EST. Numbers in parentheses represent cleavage sites for chloroplast transit peptides or secretion signals as determined with ChloroP v. 1.1 and SignalP v. 3.0, respectively. [d] Biological role of the identified protein: Ox, oxidative; Def, defense; Exp, gene/protein expression; Met, primary/secondary metabolism; ST, signal transduction; and ND, not determined. [e] Relative expression in comparison to mock-inoculated control for resistant line at 2 (R2) and 5 dpi (R5) and susceptible line at 2 (S2) and 5 dpi (S5). Increased expression (induction), +; decreased expression (repression), –; and no difference in expression level, ND.

1), is an additional protein peripherally associated with resistance. A tetratricopeptide repeat domain protein (#192), β-glucanase (#43), chitinase (#105), and syringopeptin synthetase C (#639, **Table 2**) were identified using MS/MS spectra alone. Lastly, terpene synthase (#188), PR-protein P69G (#205), ribosome inactivating protein (#27), phytoalexin deficient protein 4-2 (#129), and another β-glucanase (#639, **Table 3**) were identified by a homology-based search of NCBI. The relative abundance of resistance- (**Figure 2**) and susceptibility- (**Figure 3**) associated defense-related proteins was determined.

Stress Response Proteins. Tonoplast aquaporin (#107) was stress response-related protein identified with a combined MS + MS/MS spectra search (**Table 1**). Others identified using PEAKS-derived amino acid sequences were two abscisic acid (ABA)-induced proteins (#112, #193, **Table 3**). The relative abundance of resistance- (**Figure 2**) and susceptibility- (**Figure 3**) associated stress-related proteins was determined.

Proteins Associated with Gene Expression and Protein Turnover. Several proteins identified are involved with gene expression and protein turnover. The MS + MS/MS searches identified the following: three protein fractions as 50S ribosomal protein L12 (#24, #191, #210), ubiquitin (#12), cyclophilin (#37), and a BZIP transcription factor (#122, **Table 1**). Searches using MS/MS spectra alone identified the following: a pentatricopeptide repeat–repeat protein (#4), 60S ribosomal protein L27 (#108), and elongation factor 1α (#124, **Table 2**). Lastly, a homology-based search of an amino acid sequence derived from MS/MS spectra identified a WD-40 domain protein (#111, **Table 3**).

Metabolic Proteins. Many proteins associated with primary and secondary metabolic processes were affected by F-19 challenge. These include an ATPase (#102) and an ATP synthase confirmed with MS + MS/MS spectra (**Table 1**); biotin carboxylase (#88), β-fructofuranosidase (#182), and phosphoglycerate mutase (#209) identified with MS/MS spectra alone; and a sterol methyltransferase (#103), an adenosylmethionine transporter (#110), malate dehydrogenase (#130), CP12 (#638), acetyl CoA carboxylase (#641), and a dehydrogenase (#643) by a homology-based search of NCBI (**Table 3**).

Cell Development-Related Proteins. Four proteins identified are related to cell division, development, and modification: an actin-binding protein (#100, **Table 1**) and aurora kinase 2 splicing variant (#27), pectinesterase-like protein (#33), and pectinacetyltransferase (#130, **Table 3**).

Signal Transduction Proteins. Signal transduction-related proteins included the following kinases: two receptor-like kinases (#114, **Table 1**; #15, **Table 2**) and a wall-associated kinase (#128, **Table 3**). Another protein related to signal transduction was calmodulin (#191, **Table 2**).

Other Proteins. There were a significant number of proteins identified in this study that had homology to proteins with unknown functions including sequences predicted to be functional proteins (#18, **Table 1**; #101, #105, #131, **Table 2**; #43, #133, #195, #640, **Table 3**) and several matches to ESTs (#43, #103, #639, **Table 2**).

DISCUSSION

F. oxysporum is a major threat in sugar beet production. Currently, it is unknown why sources of resistance to the pathogen vary by geographic location. This is due in part to the lack of understanding of the basis for resistance. Dissection of the protein changes associated with resistance and susceptibility will provide a better understanding of the resistance mechanism and the biology of disease; both offer a platform for developing more effective disease control strategies. Ulti-

Table 3. Proteins in Sugar Beet Affected by Challenge with *F. oxysporum* Isolate F-19 as Identified Homology-Based Searches with PEAKS-Derived Amino Acid Sequence

peak no.	protein name	pI (obs/exp)[a]	accession no.	sequence derived[a]	sequence matched[b]	conserved domain[c]	cellular location[d]	role[e]	R2[f]	R5[f]	S2[f]	S5[f]
				resistant germplasm								
188	kaurene/terpene synthase	5.68–5.98/5.23	125582573	LLPEEVVR	LLPEEVVR	Terpene_cyclase_plant_C1	O	Def	ND	+	ND	ND
191	calmodulin-like protein	5.27–5.39/4.31 (4.27)	7801694	VLTSLGLK	VMTSLGLK	Efh	S (20/21)	ST	+	+	ND	ND
193	ABA/WDS induced protein	4.77–5.07/5.15	92874981	ELAAVGAVGAGGFAFHEHH	EVAAVAAVGSGGFAFHEHH	ABA_WDS	O	SR	+	+	ND	ND
195	stem-specific protein	<4.0/3.56	55416175	EEAAPAPAPAEVEAGPTTDR	EEAAPAPAEAEPAAVPEEAA	no CDD	O	ND	+	+	+	+
205	PR-protein P69G	5.56–5.87/6.42 (6.24)	3183991	LHSTHNPSFLG	LHTTHTPSFLG	Subtilisin_N	S (22/23)	Def	+	+	ND	ND
				susceptible germplasm								
27	ribosome inactivating protein	>8.5/9.40(9.35)	116248471	QVDSNAGNR	QIESNAGTNR	RIP	S (26/27)	Def	+	ND	+	+
27	aurora kinase 2 splicing variant	>8.5/9.08	121582248	LTFLPLEVVESGDH	LDYLPPEMVESVEHDA	S_TKc	O	CD	+	ND	+	+
33	pectinesterase-like protein	>8.5/8.53	62321360	EFVNYGP	EFMNYGP	Pectinesterase	O	CD	ND	ND	–	–
43	unknown	<4.0/4.82	115445195	YPDDFNGELVDLAMDSK	YPNDFNSGELRDL	no CDD	O	ND	+	+	ND	+
103	sterol 24-C methyltransferase	>8.5/9.66(8.97)	116056738	VGGPLR	VGGPLR	UbiE	CP (71/72)	Met	ND	ND	–	–
110	adenosylmethionine transporter	8.2–8.4/9.53	119391875	AGYRKFLVDLP	AGYRSFLLRDLP	Mito_carr	O	Met	ND	ND	–	–
111	WD-40 domain	8.2–8.4/9.02(9.04)	125572214	FSLVAR	FSLVAR	WD40	CP (62/63)	Exp	ND	ND	–	–
112	ABA ripening protein	6.70–7.0/5.33	38532363	AAAAVGANYAFHEHHEK	AAAAVGAGGYAFHEHHEK	ABA_WDS	O	SR	+	ND	–	–
115	catalase	6.12–6.42/6.39	126022836	LTVGPRG	LTVGPRG	catalase	O	Ox	ND	ND	–	–
128	wall-associated kinase	4.62–4.93/5.66(5.66)	13486777	CLGMPWCSEDRPS	CLDM--CSENRPS	S_TKc	S (20/21)	ST	ND	ND	–	–
129	phytoalexin-deficient 4-2 protein	4.62–4.93/6.49	58826319	EPLPDDAEYYR	EPL-DIAEYYR	Lipase_3	O	Def	–	–	+	ND
130	malate dehydrogenase	4.32–4.62/6.61(6.17)	125604343	DTGLDGDFELVDLAMSDK	DGDYELVKDVAMDD	Mdh	M (43/44)	Met	–	–	–	–
130	pectin acetyltransferase	4.32–4.62/6.16(5.91)	110289537	DFMLFHCSAASHNMVWRV	DFLVFDRLHCTAANR---WRV	PAE	S (23/24)	CD	ND	ND	–	–
133	unknown	<4.0/6.21(6.16)	125602214	LPDMPWAQNSTV	LPDMPWA--SSV	no CDD	M (16/17)	ND	ND	ND	–	–
638	CP12	4.32–4.62/4.81(4.16)	1617213	DVVEEVSAAASHAR	DVVEELSAAASHAR	CP12	CP (48/49)	Met	ND	ND	ND	+
639	endo-β-1,4-glucanase	>8.5/8.52(8.59)	1655543	QGWYHCPDSEGFFSSDN	QGWSQCP-SE--FSWDN	Glyco_hydro_9	S (23/24)	Def	+	ND	+	+
640	orf100f	>8.5/9.92	9838463	CSKYLR	CSKYLR	no CDD	O	ND	+	ND	ND	+
641	acetyl CoA carboxylase	4.03–4.14/4.97	108796668	HLEMGSTE	HLEMSSTE	AccD	O		+	ND	ND	+
643	dehydrogenase	>8.5/8.85	125546451	HDGQDVDTWSDR	HQGQDVD-RSDR	adh_short	O	Met	+	+	ND	+

[a] The amino acid sequence was derived from the MS/MS spectral data by PEAKS. Only amino acids identified with greater than 90% confidence were included in the homology-based search. [b] The amino acid sequence with the highest degree of homology to the PEAKS-generated sequence. [c] Denotes the name of the conserved domain where the matching amino acid peptide sequence is contained in the best match protein as determined with NCBI's conserved domain database. No CDD (no conserved domain detected) is the designation given for proteins that lacked any conserved domains. Protein identifications made in which the peptide sequence did not fall within the conserved domain were disregarded as positive matches in the scope of this study. [d] Cellular location of the identified protein was determined using TargetP v. 1.1. Location designations: M, mitochondria; CP, chloroplast; S, secreted; and O, other. Numbers in parentheses represent cleavage sites for mitochondrial transit peptide, chloroplast transit peptide, or secretion signal as determined with MITOPROT, ChloroP v. 1.1, or SignalP v. 3.0, respectively. [e] Biological role of the identified protein: Def, defense; Met, primary/secondary metabolism; CD, cell development; Exp, gene/protein expression/regulation; Ox, oxidative response related; ST, signal transduction; SR, stress related; and ND, not determined. [f] Relative expression in comparison to mock-inoculated control for resistant line at 2 (R2) and 5 dpi (R5) and susceptible line at 2 (S2) and 5 dpi (S5). Increased expression (induction), +; decreased expression (repression), –; and no difference in expression level, ND.

mately, expression differences and polymorphisms that exist between resistant and susceptible genotypes may be exploited to identify new sources of resistance with greater speed and accuracy.

Protein identification involving mass spectrometry is subject to different limitations. Many proteins in the current study were unable to be identified, based on low abundance of the protein or lack of correlation between the acquired spectra and proteins in the public database. This was not surprising since protein identification becomes increasingly difficult when analyzing proteins from poorly characterized systems, such as sugar beet. However, this type of analysis cannot be limited to well-defined model systems since host resistance and disease states are host- and pathogen-specific (*20*). Fortunately, several diverse approaches are available for identifying proteins under these circumstances and were employed in the current study. Protein identification is most accurate when corroborated with matches to several unique peptide masses and/or MS/MS spectra. Proteins identified based on a single peptide spectrum of high integrity, which may be the only detectable peptide from an enzymatic digest, can be legitimate (*21*). The legitimacy increases when the sequence is contained in a functional domain, a region highly conserved across genera (*22*). This method of single peptide–protein identification has been widely employed in plant systems (*23*–*25*). Fifty percent of the proteins analyzed by tandem MALDI-TOF/TOF could not be identified using existing genomic databases, and several identified proteins have no homology to previously characterized sequences or identifiable conserved functional domains (#18, #43, #101, #103, #105, #131, #133, #195, #639, #640). These proteins may play an integral role in plant defense, but without further information regarding function, it is difficult to follow through with hypothesis-driven science. This demonstrates the importance of the continuing genomic research in plant biology.

Protein expression in beet in response to F-19 is temporally regulated. This is consistent with transcriptomic studies of soybean response to *Fusarium* (*6*). Several proteins affected by F-19 are related to gene expression and protein turnover, including ribosomal proteins (#24, #108, #191, #210), a PPR protein (#4), a transcription factor (#122), elongation factor 1α (#124), and ubiquitin (#12). Protein expression in response to F-19 appears to come at the expense of primary (#102, #129, #130, #209, #638, #643) and secondary (#88, #103, #110, #639, #641) metabolic processes, with a majority of the effect observed in the susceptible genotype. Jonsson (*26*) noted that this type of response is more noticeable in susceptible plants since it is correlated with prolonged, widespread pathogen infection in comparison to the temporary initial defense activation in resistant lines.

In comparing the protein response of resistant and susceptible sugar beet, two striking differences were noted. First, a greater diversity of oxidative and defense-related proteins was induced in the resistant genotype, which may be responsible for resistance. Second, some stress-related factors that are potentially tied to disease are only expressed in the susceptible genotype.

The oxidative burst (OXB) is generally one of the earliest events in activation of plant resistance (*27*, *28*). It appears from the proteomic data that an oxidative reaction to F-19 is resistance-specific. A total of six proteins were identified as OEC (#1, #7, #11, resistant; #126, #128, #129, susceptible), a protein associated with resistance that generates oxygen, a substrate for superoxide anion (SO) production (*29*, *30*). Although OEC is induced in both genotypes, only the resistant genotype had coordinated expression of additional proteins necessary for the

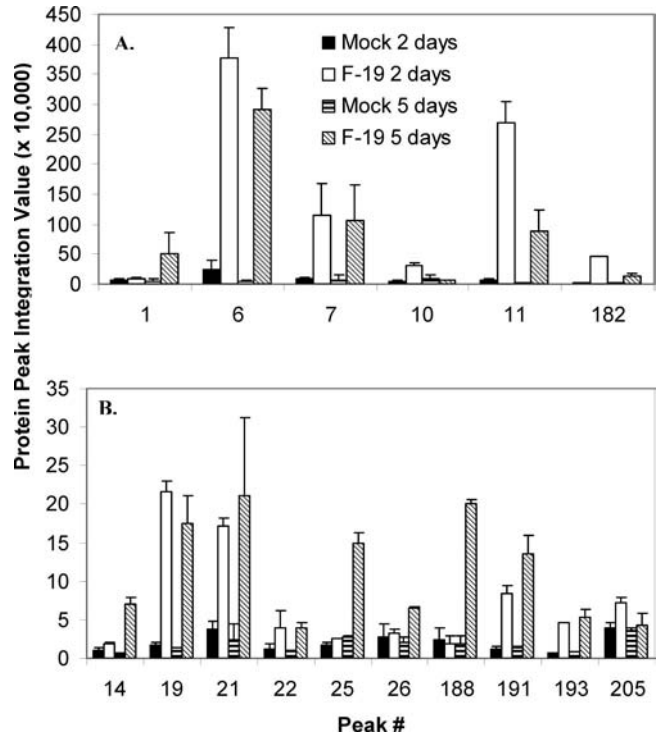

Figure 2. Relative abundance of oxidative and defense-related protein peaks differentially expressed in sugar beet genotype C1200.XH024 (resistant) following challenge with *F. oxysporum* isolate F-19 with high (**A**) and low (**B**) level expression. Results represent the average integration value (area under the protein peak detected in the 2nd dimension of MDLC) across biological replicates.

OXB (#10, #14, #21). Furthermore, a peroxisomal assembly protein (#116) and catalase (#115), two oxidative-related proteins, are repressed in the susceptible line; both are necessary for oxidative defense against fungal pathogens of tomato (*31*). Additionally, ABA-related proteins, associated with active oxygen generation (*32*), are induced in the resistant genotype (#193) and repressed in the susceptible genotype (#111, #112). Interestingly, the activity of these proteins in this capacity is reliant on calmodulin (*33*), another protein with expression limited to the resistant genotype (#191). All of these observations support the hypothesis that OXB is resistance-specific.

The mechanism of the OXB in the resistant genotype (**Figure 4**) can be inferred from the timing of expression (**Figure 2**). A SO burst is a rapid, transient response in plant disease resistance (*28*). Incidentally, the rapid, transient induction of quinone oxidoreductase (#10), a SO generator (*34*), is coincidental with this timing (**Figure 2**). Furthermore, SOD (#21), which converts SO to H_2O_2, is induced concurrently with OEC and quinone oxidoreductase, and this downstream component of the OXB remains induced at 5 dpi (**Figure 2**). Lastly, glutathione-S-transferase, the terminal enzyme in the illustrated OXB scheme (**Figure 4**), is only induced at 5 dpi and may serve as a H_2O_2 scavenger at the completion of the OXB. Future experiments include examining the role of the aforementioned proteins in free radical production.

Several classical defense-related proteins were induced in beet by F-19. Interestingly, some induction occurred regardless of host resistance or susceptibility, which is consistent with observations in other systems (*36*). Chitinase, a PR protein, was induced in both. Isozymes of this protein have had demonstrated antifungal activity in other systems (*35*) and are induced in sugar beet by other pathogens (*37*, *38*). This was likely the same isozyme in both genotypes since elution occurred at ap-

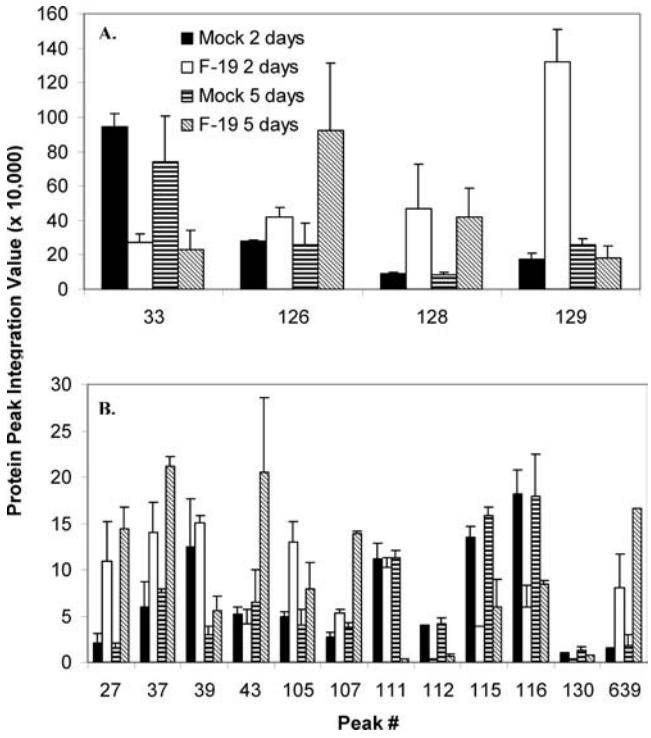

Figure 3. Relative abundance of oxidative, defense, and stress-related protein peaks differentially expressed in sugar beet genotype Fus7 (susceptible) following challenge with *F. oxysporum* isolate F-19 with high (**A**) and low (**B**) level expression. Results represent the average integration value (area under the protein peak detected in the 2nd dimension of MDLC) across biological replicates.

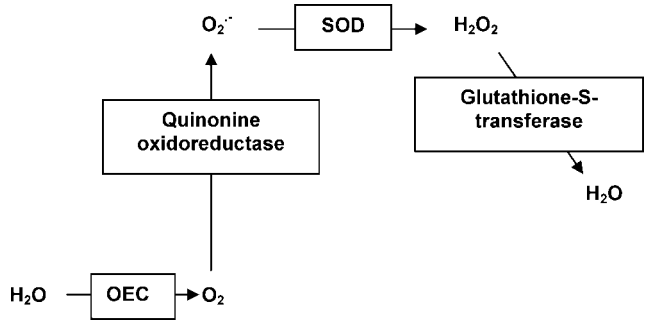

Figure 4. Hypothesized interaction of oxidative proteins in sugar beet. OEC converts water to oxygen, which could serve as a substrate for SO generation. Quinone oxidoreductase catalyzes redox reactions, which generates SO. SOD catalyzes the breakdown of SO into hydrogen peroxide, which is converted to water downstream by glutathione-S-transferase.

proximately the same pH and similar retention times (data not shown). Notably, the expression level was higher and more prolonged in the resistant genotype as compared to the, albeit significant, but transient, low level expression observed in the susceptible genotype (**Figure 3**). Peroxidase (PR-9; #39) had similar transient expression in the susceptible genotype and two other PR proteins, glucanase (#43, #639) and ribosome-inactivating protein (#27), were induced in the susceptible line but only at 5 dpi. The late and/or transient activation of these defense-related proteins may explain the lack of activity against *F. oxysporum* since timing is a critical component of plant defense (*38*). The PR proteins strictly induced in the resistant line, PR-1a (#22), PR-10 (TSI-1; #25), and PR-7 (P69G; #205), all show early and/or long-lasting induction (**Figure 2**). Additional defense-related proteins were induced only in the resistant genotype, including an allergen homologous to profilin (#19), an actin-binding protein involved in cytoskeletal dynamics that also accumulates in parsley following *Phytopthora* inoculation (*39*), and PPO (#26). Although the latter does not have a causal relationship with defense (*40*), overexpression of PPO has lead to increased resistance to bacterial infection (*41*) and insect pests (*42*) in other systems. Lastly, β-fructofuranosidase (#182), which has invertase activity and can release hexoses from sucrose for use in cell wall strengthening (*43*), a physical barrier to pathogen ingress, was only induced in the resistance genotype. In the susceptible genotype, F-19 challenge resulted in repression of pectinesterase (#33) and pectinacetyltransferase (#130), cell wall modifying enzymes (*44*). All demonstrate that a broader base of defense components is activated in the resistance line. Future plans include validating causal roles for and evaluating potential marker development using resistance-specific defense-related proteins.

Some of the susceptibility-specific proteins provide interesting clues about the disease mechanism of F-19 in sugar beet. A tonoplast aquaporin is uniquely induced in the susceptible genotype (#107). Aquaporins are proteinaceous pores that regulate water flow and solute transport (*45*). These proteins are densely packed at biotrophic interfaces and release solutes and sugar to an array of pathogens and symbiotic microorganisms (*46–48*). In the case of F-19–sugar beet interactions, aquaporins may provide food to the pathogen or be induced in response to water stress created by the pathogen plugging the vascular tissue of the root. Interestingly, regulating the expression of aquaporin through gene silencing has created increased resistance to root knot nematodes in tomato (*47*). Exploitation of similar mechanisms in beet could be explored as a novel Fusarium Yellows disease control strategy. A cyclophilin is also uniquely induced in the susceptible genotype. These proteins play important roles in fungal virulence (*49, 50*) and defense activation (*51*); therefore, future investigations into the detailed role of cyclophilin in *Fusarium* infection of sugar beet are warranted.

Characterization of protein changes associated with sugar beet resistance against and susceptibility to F-19 has provided clues about resistance and disease mechanisms. Future objectives include examining the biological relevance of the induced proteins to identify markers for resistance selection and creating new disease control strategies. Genetically modified (GM) sugar beet, in the form of glyphosate resistant beets, will be planted in commercial fields throughout the United States in 2008. The acceptance of GM beets will provide new transgenic avenues for developing novel disease tolerance. Studies, such as this, uncover resistance- and disease-specific proteins that may be suitable candidates for this approach. Of particular interest are the proteins tightly correlated with resistance in this study, which also are induced in resistant sugar beet by other pathogens, including chitinase (#6), GST (#14), PPO (#26), the major latexlike allergen (#19), and TSI-1 (#25) (*38*). Genetic modification, combined with more accurate, rapid selection of native sources of resistance, will provide a means of generating sugar beet with broad-range efficacy against a wide array of pathogenic *Fusarium* spp. and other pathogens.

ABBREVIATIONS USED

ABA, abscisic acid; DPI, days postinoculation; ESTs, expressed sequence tags; F-19, *F. oxysporum* isolate F-19; GM, genetically modified; IEX, ion exchange chromatography; MDLC, multidimensional liquid chromatography; OEC, oxygen-evolving complex; OXB, oxidative burst; PPO, polyphenol oxidase; PR, pathogenesis-related; SO, superoxide anion; SOD,

superoxide dismutase; MALDI-TOF/TOF MS, matrix-assisted laser desorption–ionization with tandem time-of-flight mass spectrometry.

ACKNOWLEDGMENT

We thank Drs. Doug Luster and Jan Leach for their critical review of the manuscript and Laurie Fortis for her technical assistance in the project.

LITERATURE CITED

(1) Curto, M.; Camafeita, E.; Lopez, J. A.; Maldonado, A. M.; Rubiales, D.; Jorrin, J. V. A proteomic approach to study pea (*Pisum sativum*) response to powdery mildew (*Erysiphe pisi*). *Proteomics* **2006**, *6*, 163–174.

(2) Fobert, P. R.; Despres, C. Redox control of systemic acquired resistance. *Curr. Opin. Plant Biol.* **2005**, *8*, 378–382.

(3) Van Loon, L. C.; Rep, M.; Pieterse, C. M. Significance of inducible defense-related proteins in infected plants. *Annu. Rev. Phytopathol.* **2006**, *44*, 135–162.

(4) Xie, Z.; Chen, Z. Salicylic acid induces rapid inhibition of mitochondrial electron transport and oxidative phosphorylation in tobacco cells. *Plant Physiol.* **1999**, *120*, 217–226.

(5) De Vos, M.; Van Oosten, V. R.; Van Poecke, R. M.; Van Pelt, J. A.; Pozo, M. J.; Mueller, M. J.; Buchala, A. J.; Metraux, J. P.; Van Loon, L. C.; Dicke, M.; Pieterse, C. M. Signal signature and transcriptome changes of Arabidopsis during pathogen and insect attack. *Mol. Plant Microbe Interact.* **2005**, *18*, 923–937.

(6) Iqbal, M. J.; Yaegashi, S.; Ahsan, R.; Shopinski, K. L.; Lightfoot, D. A. Root response to *Fusarium solani* f.sp. glycines: Temporal accumulation of transcripts in partially resistant and susceptible soybean. *Theor. Appl. Genet.* **2005**, *110*, 1429–1438.

(7) Beyer, A.; Hollunder, J.; Nasheuer, H. P.; Wilhelm, T. Post-transcriptional expression regulation in the yeast *Saccharomyces cerevisiae* on a genomic scale. *Mol. Cell. Proteomics* **2004**, *3*, 1083–1092.

(8) Shaffer, K. L.; Sharma, A.; Snapp, E. L.; Hegde, R. S. Regulation of protein compartmentalization expands the diversity of protein function. *Dev. Cell.* **2005**, *9*, 545–554.

(9) O'Brian, C. A.; Chu, F. Post-translational disulfide modifications in cell signaling—Role of inter-protein, intra-protein, S-glutathionyl, and S-cysteaminyl disulfide modifications in signal transmission. *Free Radical Res.* **2005**, *39*, 471–480.

(10) Zhao, Y.; Ramakrishnan, A.; Kim, K. E.; Rabson, A. B. Regulation of Bcl-3 through interaction with the Lck tyrosine kinase. *Biochem. Biophys. Res. Commun.* **2005**, *335*, 865–873.

(11) Zuo, X.; Speicher, D. W. A method for global analysis of complex proteomes using sample prefractionation by solution isoelectric focusing prior to two-dimensional electrophoresis. *Anal. Biochem.* **2000**, *284*, 266–278.

(12) Barnea, E.; Sorkin, R.; Ziv, T.; Beer, I.; Admon, A. Evaluation of prefractionation methods as a preparatory step for multidimensional based chromatography of serum proteins. *Proteomics* **2005**, *5*, 3367–3375.

(13) Cooper, J. W.; Wang, Y.; Lee, C. S. Recent advances in capillary separations for proteomics. *Electrophoresis* **2004**, *25*, 3913–3926.

(14) Wang, Y.; Balgley, B. M.; Lee, C. S. Tissue proteomics using capillary isoelectric focusing-based multidimensional separations. *Exp. Rev. Proteomics* **2005**, *2*, 659–667.

(15) Guttman, A.; Varoglu, M.; Khandurina, J. Multidimensional separations in the pharmaceutical arena. *Drug Discovery Today* **2004**, *9*, 136–144.

(16) Harveson, R. M.; Rush, C. M. Genetic variation among *Fusarium oxysporum* isolates from sugar beet as determined by vegetative compatibility. *Plant Dis.* **1997**, *81*, 85–88.

(17) Hanson, L. E.; Hill, A. L. *Fusarium* species causing Fusarium yellows of sugarbeet. *J. Sugarbeet Res.* **2004**, *41*, 163–178.

(18) Ma, B.; Zhang, K.; Hendrie, C.; Liang, C.; Li, M.; Doherty-Kirby, A.; Lajoie, G. PEAKS: Powerful software for peptide de novo sequencing by MS/MS rapid commun. *Mass Spectrom.* **2003**, *17*, 2337–2342.

(19) Zhou, W.; Eudes, F.; Laroche, A. Identification of differentially regulated proteins in response to a compatible interaction between the pathogen *Fusarium graminearum* and its host *Triticum aestivum*. *Proteomics* **2006**, *6*, 4599–4609.

(20) Stout, M. J.; Workman, K. V.; Bostock, R. M.; Diffey, S. S. Specificity of induced reistance in the tomato *Lycopersicon esculentum*. *Oecologia* **1998**, *113*, 74–81.

(21) Rohrbough, J. G.; Breci, L.; Merchant, N.; Miller, S.; Haynes, P. A. Verification of single-peptide protein identifications by the application of complementary database search algorithms. *J. Biomol. Technol.* **2006**, *17*, 327–332.

(22) Hannenhalli, S. S.; Russell, R. B. Analysis and prediction of functional sub-types from protein sequence alignments. *J. Mol. Biol.* **2000**, *303*, 61–76.

(23) Lippert, D.; Chowrira, S.; Raph, S. G.; Zhuang, J.; Aeschliman, D.; Ritland, C.; Ritland, K.; Bohlmann, J. Conifer defense against insects: Proteome analysis of Sitka spruce (*Picea sitchensis*) bark induced by mechanical wounding or feeding by white pine weevils (*Pissodes strobe*). *Proteomics* **2007**, *7*, 248–270.

(24) Ferreira, S.; Hjernok, K.; Larsen, M.; Wingsle, G.; Larsen, P.; Fey, S.; Roepstorff, P.; Salome Pais, M. Proteome profiling of *Populus euphratica* Oliv. upon heat stress. *Ann. Bot.* **2006**, *98*, 361–377.

(25) Hajheidari, M.; Abdollahian-Noghabi, M.; Askari, H.; Heidari, M.; Sadeghian, S. Y.; Ober, E. S.; Salekdeh, G. H. Proteome analysis of sugar beet leaves under drought stress. *Proteomics* **2005**, *5*, 950–960.

(26) Jonsson, U. A conceptual model for the development of Phytopthora disease in *Quercus robur*. *New Phytol.* **2006**, *171*, 55–67.

(27) Asada, K. The water-water cycle in chloroplasts: scavenging of active oxygens and dissipation of excess photons. *Annu. Rev. Plant Physiol. Plant Mol. Biol.* **1999**, *50*, 601–639.

(28) Lamb, C.; Dixon, R. A. The oxidative burst in plant disease resistance. *Annu. Rev. Plant Physiol. Plant Mol. Biol.* **1997**, *48*, 251–275.

(29) Abbink, T. E. M.; Peart, J. R.; Mos, T. N. M.; Baulcombe, D. C.; Bol., J. F.; Linthorst, H. J. M. Silencing of a gene encoding a protein component of the oxygen-evolving complex of photosystem II enhances viral replication in plants. *Virology* **2002**, *295*, 307–319.

(30) Yang, C.-W.; Gonzalez-Lamothe, R.; Ewan, R. A.; Rowland, O.; Yoshioka, H.; Shenton, M.; Ye, H.; O'Donnell, E.; Jones, J. D. G.; Sadanandom, A. The E3 ubiquitin ligase activity of Arabidopsis PLANT U-BOX17 and its functional tobacco homolog ACRE276 are required for cell death and defense. *Plant Cell* **2006**, *18*, 1084–1098.

(31) Kuzniak, E.; Sklodowska, M. Fungal pathogen-induced changes in the antioxidant systems of leaf peroxisomes from infected tomato plants. *Planta* **2005**, *222*, 192–200.

(32) Hu, X.; Jiang, M.; Zhang, A.; Lu, J. Abscisic acid-induced apoplastic H_2O_2 accumulation up-regulates the activities of chloroplastic and cytosolic antioxidant enzymes in maize leaves. *Planta* **2005**, *223*, 57–68.

(33) Hu, X.; Jiang, M.; Zhang, J.; Zhang, A.; Lin, F.; Tan, M. Calcium-calmodulin is required for abscisic acid-induced antioxidant defense and functions both upstream and downstream of H_2O_2 production in leaves of maize (*Zea mays*) plants. *New Phytol.* **2007**, *173*, 27–38.

(34) O'Brien, P. J. Molecular mechanisms of quinone cytotoxicity. *Chem.-Biol. Interact.* **1991**, *80*, 1–41.

(35) Li, C.; Bai, Y.; Jacobsen, E.; Visser, R.; Lindhout, P.; Bonnema, G. Tomato defense to the powdery mildew fungus: Differences in expression of genes in susecptible, monogenic- and polygenic resistance responses are mainly in timing. *Plant Mol. Biol.* **2006**, *62*, 127–140.

(36) Shenoy, S. R.; Kameshwari, M. N.; Swaminathan, S.; Gupta, M. N. Major antifungal activity from the bulbs of Indian squill *Urginea indica* is a chitinase. *Biotechnol. Prog.* **2006**, *22*, 631–637.

(37) Nielsen, K. K.; Mikkelsen, J. D.; Kragh, K. M.; Bojsen, K. An acidic class III chitinase in sugar beet: Induction by *Cercospora beticola*, characterization, and expression in transgenic tobacco plants. *Mol. Plant Microbe Interact.* **1993**, *6*, 495–506.

(38) Puthoff, D. P.; Smigocki, A. C. Insect feeding-induced differential expression of *Beta vulgaris* root genes and their regulation by defense-associated signals. *Plant Cell Rep.* **2007**, *26*, 71–84.

(39) Schutz, I.; Gus-Mayer, S.; Schmelzer, E. Profilin and Rop GTPases are localized at infection sites of plant cells. *Protoplasma* **2006**, *227*, 229–235.

(40) Mayer, A. M. Polyphenol oxidase in plants and fungi: going places? A review. *Phytochemistry* **2006**, *67*, 2318–2331.

(41) Li, L.; Steffans, J. C. Overexpression of polyphenol oxidase in transgenic tomato plants results in enhanced bacterial disease resistance. *Planta* **2002**, *215*, 239–247.

(42) Wang, J.; Constabel, C. P. Polyphenol oxidase overexpression in transgenic Populus enhances resistance to herbivory by forest tent caterpillar (*Malacosoma disstria*). *Planta* **2004**, *220*, 87–96.

(43) Zhang, L.; Cohn, N. S.; Mitchell, J. P. Induction of a pea cell-wall invertase gene by wounding and its localized expression in phloem. *Plant Physiol.* **1996**, *112*, 1111–1117.

(44) Gaffe, J.; Tiznado, M. E.; Handa, A. K. Characterization and functional expression of a ubiquitously expressed tomato pectin methylesterase. *Plant Physiol.* **1997**, *114*, 1547–1556.

(45) Tyerman, S. D.; Niemietz, C. M.; Bramley, H. Plant aquaporins: multifunctional water and solute channels with expanding roles. *Plant Cell Environ.* **2002**, *25*, 173–194.

(46) Smith, S. E.; Dickson, S.; Smith, F. A. Nutrient transfer in arbuscular mycorrhizas: how are fungal and plant processes integrated. *Aust. J. Plant Physiol.* **2001**, *28*, 683–694.

(47) Oppermann, C. H.; Taylor, C. G.; Conkling, M. A. Root-knot nematode-directed expression of a plant root-specific gene. *Science* **1994**, *263*, 221–223.

(48) Bird, D. M. Manipulation of host gene expression of root-knot nematodes. *J. Parasitol.* **1996**, *82*, 881–888.

(49) Viaud, M. C.; Balhadere, P. V.; Talbot, N. J. A Magnaporthe grisea cyclophilin acts as a virulence determinant during plant infection. *Plant Cell* **2002**, *14*, 917–930.

(50) Viaud, M.; Brunet-Simon, A.; Brygoo, Y.; Pradier, J. M.; Levis, C. Cyclophilin A and calcineurin functions investigated by gene inactivation, cyclosporine A inhibition and cDNA arrays approaches in the phytopathogenic fungus *Botrytis cinerea*. *Mol. Microbiol.* **2003**, *50*, 1451–1465.

(51) Coaker, G.; Zhu, G.; Ding, Z.; Van Doren, S. R.; Staskawicz, B. Eukaryotic cyclophilin as a molecular switch for effector activation. *Mol. Microbiol.* **2006**, *61*, 1485–1496.

Received for review March 26, 2007. Revised manuscript received July 17, 2007. Accepted July 17, 2007.

JF070876Q